

## Local-field method for resistivity and electromigration in metallic microstructures: Application to thin films

C. S. Chu and R. S. Sorbello

*Department of Physics and Laboratory for Surface Studies, University of Wisconsin-Milwaukee, Milwaukee, Wisconsin 53201*

(Received 10 February 1988; revised manuscript received 1 June 1988)

A local-field method is described for determining the microscopic potential, the electrical resistivity, and the electromigration driving force on an impurity in a metallic microstructure. The method is an extension of Landauer's picture of residual-resistivity dipoles to microstructures, with greater emphasis placed upon the details of the quantum-mechanical scattering process. Using a microscopic, surface-impurity model for surface roughness, we apply the method to a metallic thin film. When the film thickness is smaller than the mean free path, the surface resistivity is found to have oscillatory behavior as a function of film thickness. The form of the oscillations depends upon multiple scattering between the surface impurity and the film surfaces. In thicker films, the Fuchs-Sondheimer result is recovered. The local potential set up by impurity scattering is dipolar in the near- and far-field regions. However, unlike the case of residual-resistivity dipoles in bulk, the effective dipole strength is generally different in the two regions. It is found that the residual-resistivity dipole field decays less rapidly with distance in a thin film than in bulk, thus resulting in a larger voltage drop across an impurity in a thin film. This field enhancement is expected in low-dimensional systems.

### I. INTRODUCTION

Electron transport in metallic microstructures has received increasing theoretical and experimental attention in the past decade.<sup>1</sup> These microstructures typically have at least one of their characteristic dimensions smaller than the electron mean free path, and as a result electrons can undergo coherent multiple scattering between interfaces as well as between interfaces and defects. In this quantum interference regime, the dc transport coefficients are expected to be very sensitive to the configuration of defects and to the structure of the interfaces. A particular configuration of defects will give rise to a characteristic local electric field and current distribution on a microscopic level.<sup>2-7</sup>

The resistivity of a metallic microstructure can be formally expressed in terms of the transmission coefficient according to the Landauer formula.<sup>8</sup> This formula has been the basis of extensive model calculations for the resistivity due to a random distribution of impurities in one-dimensional systems.<sup>9</sup> Recently we described a general local-field method for calculating the impurity resistivity of an arbitrary metallic microstructure,<sup>6</sup> and we applied the method to a two-dimensional system,<sup>6</sup> a semi-infinite system<sup>6</sup> and a thin film in which electrons occupy only the lowest subband.<sup>7</sup> This local-field method does not involve the Landauer formula *per se*, nor its multi-channel generalization.<sup>10</sup> However, in common with the Landauer formula approach, the local-field method is based on ideas contained in Landauer's seminal 1957 paper on the spatial variation of currents and fields due to localized scatterers. Essentially, the local-field method which we employ is an extension of Landauer's picture to microstructures, with greater emphasis placed upon the de-

tails of the quantum mechanical scattering process. Such details can be of crucial importance for microstructures, especially when impurities are situated near interfaces.

The local-field method provides a tractable scheme for determining the microscopic potential, the electrical resistivity, and the electromigration driving force on an impurity in the microstructure. Electromigration is the phenomenon of impurity migration in the presence of an electric field and the accompanying electron current.<sup>11-17</sup> Effectively, the impurities are driven by the local microscopic electric field.<sup>4,5</sup>

According to Landauer,<sup>2,3</sup> the increase in resistivity due to an impurity is associated with a microscopic dipolar source of electric field and current. This dipolar source is called the residual resistivity dipole (RRD). The RRD is not only a useful concept for the formulation of electron transport in microstructures, but is also important for understanding the detailed nature of the local field. An effective RRD can also be defined when the scatterer or a group of scatterers is in the neighborhood of interfaces of a microstructure, provided that the size of the scatterer group is not larger than the background mean free path  $l$ . To understand how the RRD field is set up due to the scatterers, we consider a scatterer group in the vicinity of interfaces of a microstructure. The center of this scatterer group is at location  $\mathbf{R}$ . When electrons are scattered by the scatterer group and arrive at another position, say  $\mathbf{r}$ , there is a local pile-up of charges and the local potential is adjusted so as to neutralize the excess space charges. The local potential shift is the RRD field. It is then clear that for  $|\mathbf{r}-\mathbf{R}| < l$ , the local potential depends on the quantum mechanical scattering by the group and interfaces. When  $|\mathbf{r}-\mathbf{R}| > l$ , the local potential depends also on the background scattering, which we

assume is incoherent in nature. The calculation of the local electrostatic potential is then divided into two regimes, namely, the near-field regime (region close to the scatterer group) and the far-field regime (region far from the scatterer group). This idea of considering the local potential in two regimes is also contained in Landauer's paper.<sup>2</sup>

The definition of the resistivity or resistance of a microstructure requires some care. The resistance as inferred from a measurement of voltage depends upon the position of the voltage probes. When the distance between probes is smaller than  $l$ , the measured voltage and the inferred resistivity are governed by quantum mechanical interference phenomena involving defects, interfaces and, in general, the probes themselves. This is the situation in recent experiments<sup>18,19</sup> which have probed the voltage drop across defects in a microstructure. On the other hand, if the distance between probes is larger than  $l$ , we are outside the quantum interference regime. The measured voltage is no longer sensitive to the precise position of the probes, although particular scatterer groups between the probes may still undergo strong multiple scattering and exhibit quantum interference effects. In any case, knowledge of the local potential and the probe configuration would allow the appropriate resistivity to be calculated.

In addition to the local field and resistivity, we also consider the electromigration force. The driving force for electromigration in a highly conducting metal arises largely due to the "electron wind force," that is, the momentum transfer by the electrons to the impurity atom.<sup>11</sup> It turns out that the wind force, resistivity and RRD are closely related to one another. In this paper, we describe a local field method for calculating the wind force, the local potential and the resistivity of an arbitrary metallic microstructure. We then apply the method to the thin film case.

The resistivity of a thin metal film exhibits a "size effect",<sup>20-28</sup> or depends on film thickness  $d$ , when  $d$  is smaller than or comparable to  $l$ . For even thinner metal films, i.e., when  $\lambda_F \gtrsim d$ , where  $\lambda_F$  is the de Broglie wavelength of electrons at the Fermi level of the corresponding bulk material, the "quantum size effect" becomes important. (Actually, when  $d$  is several times  $\lambda_F$ , quantum interference is already important, as we shall see.) In the quantum size effect regime, the electron momentum is quantized and the quantum interference phenomena are expected to be more pronounced.

The earliest theoretical attempts to describe the size effect in metal films were by Fuchs<sup>23</sup> and Sondheimer.<sup>24</sup> They defined a specular parameter  $p$  in order to set up a simple boundary condition on the distribution function  $f$ , which they then obtained by solving the Boltzmann equation subject to their boundary condition. The value of  $p$  ranged from  $p=1$  (totally specular reflection) to  $p=0$  (totally diffuse surface scattering). Soffer<sup>25</sup> extended the theory to obtain  $p$  from a statistical model for surface roughness. His theory, however, is basically a semiclassical one which is adequate only for thicker films.<sup>26-28</sup> For thin films ( $d < l$ ), the variation of  $f$  along the thickness of the film is somewhat ill defined, and there is doubt about

the validity of solving the Boltzmann equation with  $z$ -dependence in  $f$  to match the boundary condition, where  $z$  is the coordinate perpendicular to the film.

Recently, Leung<sup>29</sup> and Tešanović *et al.*<sup>30</sup> have calculated the resistivity of metallic thin films in the quantum interference regime. In the paper by Leung,<sup>29</sup> the interfaces are characterized by a Gaussian distribution function and, keeping the effect of surface roughness to leading order, he finds that the resistivity of the thin film has oscillatory behavior as a function of  $d$ . In the paper by Tešanović *et al.*,<sup>30</sup> the interfaces are characterized by a "white noise" surface profile which may describe an uncorrelated, atomically rough surface and the resistivity is found to increase monotonically with decreasing  $d$ . Further study is called for, both theoretical and experimental, to resolve this controversial behavior of the resistivity in thin metal films. In this paper, we apply the local-field method to an atomistic model of surface roughness, and calculate the resulting resistivity of a thin metal film.

The outline of this paper is as follows. In Sec. II, we introduce the local-field method to calculate the resistivity of arbitrary microstructures for scatterer groups near the interfaces of these microstructures. The local potential that is set up around the localized scatterer in the quantum mechanical asymptotic region is found. The corresponding local potential in the far-field region, i.e., when the distance from the scatterer is larger than  $l$ , can be found by solving a Boltzmann equation with a localized source term. The source term, which arises from the electrons scattered out by the impurity, can be determined from the full quantum-mechanical scattering problem. An expression for the wind force is also given. In Sec. III, we apply the method to a continuous metal film. The resistivity due to  $s$ -wave impurities in a film with flat boundaries is calculated. A microscopic model for the surface roughness is proposed by locating the impurities near the surface of the film. The resulting surface resistivity shows oscillatory behavior, similar to the result of Leung.<sup>29</sup> The oscillatory behavior is caused by discrete jumps in the density of states and by multiple scattering between an impurity and the film boundaries. As far as we are aware, this is the first calculation of thin film resistivity in which surface roughness is described by an atomistic model which includes multiple scattering effects between an impurity and the surfaces. Sec. IV presents a discussion and conclusion.

## II. GENERAL FRAMEWORK

We consider a metallic microstructure connected to two highly conducting leads, one to the left-hand side and the other to the right-hand side of the microstructure. The microstructure can be a thin film, thin wire or even a superlattice. The leads are connected to electron reservoirs which supply electrons to, and drain electrons from, the microstructure. For simplicity we assume that the leads are made of the same material as the microstructure (i.e., they have the same electron density and the same mean free path due to background scattering). The microstructure itself contains additional impurities. The quantity of interest here is the additional resistivity,  $\Delta\rho$ ,

due to these impurities.

For the present, consider the case of a microstructure containing only a single impurity cluster, or scatterer group, whose size is characterized by the length  $L$ , where  $L < l$ . The electrons incident upon the scatterer group are described by a shifted Fermi distribution which is set up by the background scattering that occurs in the leads and in the region of the microstructure far from the scatterer group. Assuming a free-electron-like bulk material, the part of the incident distribution that is out of static equilibrium is

$$g_{\mathbf{k}}^0 = -\tau e \mathbf{v}_{\mathbf{k}} \cdot \mathcal{E}_0 \delta(\epsilon_{\mathbf{k}} - E_F), \quad (1)$$

where  $\tau$  is the electronic relaxation time associated with background scattering processes,  $\mathcal{E}_0$  is the uniform macroscopic electric field in the absence of the scatterer group,  $\mathbf{v}_{\mathbf{k}} = \hbar \mathbf{k} / m$  is the electron velocity,  $\epsilon_{\mathbf{k}} = \hbar^2 k^2 / 2m$  is the electron energy,  $E_F$  is the Fermi energy,  $m$  is the electron mass and  $e$  is the magnitude of the charge of the electron. The net particle current arising from the distribution in Eq. (1) is given by  $\mathbf{J}_0 = -n_0 e \tau \mathcal{E}_0 / m$ , where  $n_0$  is the average density of conduction electrons in the microstructure. The net current consists of an excess of electrons moving antiparallel to  $\mathcal{E}_0$  and a deficit of electrons flowing parallel to  $\mathcal{E}_0$ , with each component contributing an amount  $\frac{1}{2} \mathbf{J}_0$  to the current density.

Each of the electron states  $\mathbf{k}$  within the incident distribution  $g_{\mathbf{k}}^0$  represents an incident electron wave that will be scattered by the scatterer group. We shall determine the scattered waves by solving the appropriate quantum mechanical scattering problem. From the scattered waves we then obtain the charge density and the local potential field.

Thus far we have considered a single localized scatterer group within a microstructure. If there are neighboring groups we shall assume that they are sufficiently separated so that they scatter electrons independently. Thus the electron distribution that is incident upon any group, after scattering by background incoherent scattering processes and by neighboring groups, is assumed to have recovered to the form given in Eq. (1). Effectively, the scatterer groups are being considered in the dilute limit.

We now turn to the calculation of the local potential and the electromigration driving force associated with a scatterer group in the microstructure. As mentioned in Sec. I, the calculation can be separated into two regimes: namely, the near-field regime  $r < l$  and the far-field regime  $r > l$ , where  $r$  is the distance measured from the center of the scatterer group. The former case requires a full quantum-mechanical scattering treatment. The latter case defines a Boltzmann-type transport problem. Since the electromigration force depends only on the local scattering environment, the electromigration driving force can be found from consideration of the  $r < l$  regime.

#### A. Near-field region

In the near-field region, the general method is the following: First, we calculate the scattered wave function  $\psi_{\mathbf{k}}^{(+)}(\mathbf{r})$  for each electron incident in the plane-wave state  $\psi_{\mathbf{k}}^0(\mathbf{r})$  within the microstructure. Second, we compute the

perturbed electron density,  $\delta n_w(\mathbf{r})$ , due to the electron current (or "electron wind"). It is given by<sup>2,3,5,15</sup>

$$\delta n_w(\mathbf{r}) = \sum_{\mathbf{k}} g_{\mathbf{k}}^0 |\psi_{\mathbf{k}}^{(+)}(\mathbf{r})|^2. \quad (2)$$

Third, we determine the corresponding self-consistent electrostatic potential  $\delta\Phi(\mathbf{r})$  from the screening relation<sup>2,3,5</sup>

$$\delta\Phi(\mathbf{r}) = -\frac{\delta n_w(\mathbf{r})}{e(dn/dE)}, \quad (3)$$

where  $dn/dE$  is the electronic density of states at  $E_F$  in the desired region of space. We remark that the self-consistent electron density is not  $\delta n_w$ , but is  $\delta n_w + \delta n_s$ , where  $\delta n_s$  is the induced screening charge which attempts to locally neutralize  $\delta n_w$ . Although  $\delta\Phi$  in Eq. (3) is expressed in terms of  $\delta n_w$ , it actually arises from  $\delta n_w$  and  $\delta n_s$ . The microscopic electric field,  $\delta\mathcal{E}(\mathbf{r})$ , which accompanies the transport process is determined from the potential through the usual relation,  $\delta\mathcal{E}(\mathbf{r}) = -\nabla\delta\Phi(\mathbf{r})$ . Linear response is assumed throughout, i.e., only the response linear in  $\mathcal{E}_0$  is considered.

Besides giving the local field, this general method also allows us to calculate the average electron wind force on an impurity inside the scatterer group. This force equals the momentum transfer per second from the electrons to the scatterer group divided by the total number of scatterers  $N$ , in the group. The average wind force  $F_w$  becomes

$$F_w = \frac{\hbar k_F}{N} \int J_r(\hat{\mathbf{r}}) \hat{\mathbf{r}} \cdot \hat{\mathcal{E}}_0 dA, \quad (4)$$

where  $dA$  is the infinitesimal element of area perpendicular to the radial direction. (The dimensionality of  $dA$  depends on the geometry of the microstructure.) Here,  $J_r \hat{\mathbf{r}}$  is the radial scattered particle current density in the vicinity of the scatterer group and emanating from the scatterer group. It is given by

$$J_r(\mathbf{r}) = \sum_{\mathbf{k}} g_{\mathbf{k}}^0 \frac{\hbar}{m} \operatorname{Re} \left[ \frac{1}{i} \psi_{\mathbf{k}}^{(+)*}(\mathbf{r}) \frac{\partial}{\partial r} \psi_{\mathbf{k}}^{(+)}(\mathbf{r}) - \frac{1}{i} \psi_{\mathbf{k}}^{0*}(\mathbf{r}) \frac{\partial}{\partial r} \psi_{\mathbf{k}}^0(\mathbf{r}) \right]. \quad (5)$$

The radial scattered current dominates the current that is scattered in other directions in the quantum-mechanical asymptotic region where  $r \gg 1/k_F$  and  $r$  is larger than size of scatterer group. If the scatterer group becomes only one scatterer, which is the dilute impurity limit, then expression (4) gives the correct  $F_w$  on that impurity. We note our convention is that a positive  $F_w$  indicates a force in the direction opposite to  $\mathcal{E}_0$ , i.e., along the direction of the electron wind.

The local electrostatic potential will be perturbed, in general, when voltage microprobes are attached along the microstructure because of quantum interference.<sup>19</sup> In this case, we should include the microprobes as additional scatterers and solve the problem again following the procedures outlined in this section.

### B. Far-field region

The electrons incident upon the microstructure, or upon a scatterer group in the microstructure, undergo quantum mechanical multiple scattering and then leave the scatterer group before they encounter appreciable incoherent scattering or inelastic scattering. What happens thereafter is well described by a Boltzmann-type transport equation. Therefore the general method to calculate local electric fields and the resulting resistivity in this region is to write down the correct form of the Boltzmann equation, in accordance with the geometry of the microstructure, and to include a particle source term. The physical reason for including a source term is that particles scattered away from the scatterer group cannot be neglected for a correct description of the far-field effects of these scatterers.

The dynamic electron distribution  $g_{\mathbf{k}}$  satisfies the transport equation. For purposes of illustration, we consider the transport equation for the bulk case. Extension of the method to various microstructures of different geometry is straightforward and is presented for the case of a thin film in Sec. III. In the latter case the dynamic electron distribution is  $g_{n\mathbf{k}}$  rather than  $g_{\mathbf{k}}$ , where  $n$  is the subband index and  $\mathbf{k}$  becomes a wave vector parallel to the film. The transport equation for the bulk case is

$$\mathbf{v}_{\mathbf{k}} \cdot \nabla_{\mathbf{r}} g_{\mathbf{k}} + \mathbf{v}_{\mathbf{k}} \cdot e \mathcal{E}_0 \delta(\epsilon_{\mathbf{k}} - E_F) = - \frac{(g_{\mathbf{k}} - \bar{g}_{\mathbf{k}})}{\tau} + S_{\mathbf{k}}(\mathbf{r}), \quad (6)$$

where  $\bar{g}_{\mathbf{k}} = (1/4\pi) \int d\Omega_{\hat{\mathbf{k}}} g_{\mathbf{k}}$  is the local average to which the electrons relax.<sup>31</sup> The source term  $S_{\mathbf{k}}(\mathbf{r})$  in Eq. (6) can be written in the form

$$S_{\mathbf{k}}(\mathbf{r}) = \delta(\mathbf{r}) \delta(\epsilon_{\mathbf{k}} - E_F) S(\hat{\mathbf{k}}), \quad (7)$$

where the center of the scatterer group is chosen to be the origin of our coordinate system. The spatial delta function  $\delta(\mathbf{r})$  in Eq. (7) implies that the particle source is a point source, since the typical length scale,  $l$ , in Eq. (6) is considerably larger than the dimension of the scatterer group. We note that, in contrast to the conventional transport equation, the source term has retained the information about the location of the scatterer group whereas conventional transport equation uses only the ensemble averaged transition probability in the collision term.<sup>32</sup> We emphasize that the local potential  $\delta\Phi(\mathbf{r})$  does not appear as a driving field in the transport Eq. (6). Rather the effects of  $\delta\Phi(\mathbf{r})$  are properly accounted for via Eq. (3). This point was made by Landauer.<sup>2</sup>

To obtain the explicit expression for the source term in Eq. (6), we note that the rate of particles being emitted by the source within solid angle  $\Delta\Omega_{\hat{\mathbf{k}}}$  is given by

$$\frac{2}{(2\pi)^3} \int dk k^2 \int d\mathbf{r} S_{\mathbf{k}}(\mathbf{r}) \Delta\Omega_{\hat{\mathbf{k}}}.$$

But the rate can also be expressed in terms of  $J_r$  as  $J_r(\mathbf{r}) r^2 \Delta\Omega_{\hat{\mathbf{r}}} |_{\hat{\mathbf{r}}=\hat{\mathbf{k}}}$ . Therefore,  $S(\hat{\mathbf{k}})$  in Eq. (7) becomes

$$S(\hat{\mathbf{k}}) = \frac{4\pi^3 \hbar^2}{mk_F} J_r(\mathbf{r}) r^2 |_{\hat{\mathbf{r}}=\hat{\mathbf{k}}}, \quad (8)$$

and the transport equation in Eq. (6) can be solved, using

the substitution

$$g_{\mathbf{k}} = g_{\mathbf{k}}^0 + g(\hat{\mathbf{k}}, \mathbf{r}) \delta(\epsilon_{\mathbf{k}} - E_F). \quad (9)$$

The long-range ( $r > l$ ) perturbed electron density  $\delta n_w(\mathbf{r})$  follows from

$$\delta n_w(\mathbf{r}) = \frac{1}{\Omega} \sum_{\mathbf{k}} (g_{\mathbf{k}} - g_{\mathbf{k}}^0), \quad (10)$$

and the long-range electrostatic potential  $\delta\Phi(\mathbf{r})$  is given by the neutralization condition in Eq. (3). The resulting  $\delta\Phi(\mathbf{r})$  is dipolar in the region  $r \gg l$ . For the case of a single impurity,  $\delta\Phi(\mathbf{r})$  is calculated in Appendix A. The result is the usual Landauer RRD field.

The resistance of the microstructure is equal to the average potential drop across the sample divided by the transmitted current. In general, one must carefully specify the geometry and location of the probes in order to determine the appropriate potential drop. This will become clear in the remainder of the paper where we apply the general method to thin metal films. We notice that the electric field  $\mathcal{E}_0$  and  $\tau$  do not enter the final result for the impurity resistivity because both the average potential drop and the transmitted current are linear in  $\mathcal{E}_0$  and  $\tau$ . Therefore, the choice of relaxation time  $\tau$  in Eq. (1) for  $g_{\mathbf{k}}^0$  is irrelevant as far as the resistivity due to impurities is concerned.

### III. TRANSPORT IN A THIN METAL FILM

The general method outlined in Sec. II is applied to the case of a thin metal film. The film thickness  $d$  we consider is for the regime  $d \ll l$ , in which the size effect and quantum size effect are expected to be important ( $l$  is the bulk mean free path for the electron). For the thin film, we choose a coordinate system in which the origin is at the center of the film. The electrons can move along the  $xy$  plane and are confined along the  $z$  direction within  $|z| < d/2$ . The position vector is denoted by  $\mathbf{r} = \rho + z\hat{\mathbf{z}}$  where  $\rho$  is the radial distance from origin on the  $xy$ -plane and  $\phi$  is the azimuthal angle. An infinite wall is assumed for the confining potential, and an impurity is taken to lie at a distance  $b$  inside the upper surface, i.e., at  $z = d/2 - b$ . The impurity potential is assumed to be spherically symmetric and confined within a small muffin-tin radius (smaller than  $b$ ). The electrons incident upon the impurity are described by the wave functions  $\psi_{n\mathbf{k}}^0$ , which have the form

$$\psi_{n\mathbf{k}}^0(\mathbf{r}) = \sqrt{2/\Omega} \sin \left[ \frac{n\pi}{d} \left( z + \frac{d}{2} \right) \right] e^{i\mathbf{k} \cdot \rho}, \quad (11)$$

where  $n$ , a positive integer, signifies a subband solution. Here  $\mathbf{k} = (k_x, k_y)$  and  $\Omega = Ad$  is the film volume.

The scattering solution  $\psi_{n\mathbf{k}}^{(\pm)}$  which evolves from  $\psi_{n\mathbf{k}}^0$  is readily determined in our model by noting that the incident wave function in Eq. (11) can be written as

$$\psi_{n\mathbf{k}}^0(\mathbf{r}) = \frac{-i}{\sqrt{2\Omega}} (e^{i\mathbf{K}_n^{(+)} \cdot \mathbf{r} + in\pi/2} - e^{i\mathbf{K}_n^{(-)} \cdot \mathbf{r} - in\pi/2}), \quad (12)$$

where  $\mathbf{K}_n^{(\pm)} = \mathbf{k} \pm (n\pi/d)\hat{\mathbf{z}}$ . The wave function in Eq. (12) is a superposition of two plane waves. The solution for

the incident wave function scattered by the impurity in the confined film is effectively the same as the solution for the two superposed propagating waves incident upon an image-potential array in otherwise empty space. Of course, we use the image problem solutions only within the physical region  $|z| < d/2$ . The locations of the image potentials are given by  $\mathbf{R}_{j\nu} = [(2j + \frac{1}{2})d + \nu b]\hat{\mathbf{z}}$ , where  $j$  is an integer and  $\nu = \pm 1$ . The image-potential array can be grouped into unit cells, labeled by  $j$ , with two image potentials per unit cell, denoted by  $\nu$ . The lattice spacing of the array is  $2d$  (see Fig. 1).

The energy of an incident electron in state  $\psi_{n\mathbf{k}}^0$  is given by

$$E = \frac{\hbar^2 K^2}{2m} = \frac{\hbar^2}{2m} \left[ \left( \frac{n\pi}{d} \right)^2 + k^2 \right], \quad (13a)$$

where  $K \equiv |\mathbf{K}_n^{(\pm)}|$ . At the Fermi energy  $E_F$ , Eq. (13a) becomes

$$E_F \equiv \frac{\hbar^2 K_F^2}{2m} = \frac{\hbar^2}{2m} \left[ \left( \frac{n\pi}{d} \right)^2 + k_{Fn}^2 \right], \quad (13b)$$

for all occupied subbands  $n$ , i.e., for all  $n$  values such that  $E_F > (\hbar^2/2m)(n\pi/d)^2$ . Here,  $k_{Fn}$  is the effective Fermi wave vector on the  $k_x, k_y$  plane. Upon counting the occupied states of all subbands, one can readily obtain the relation

$$\sum_{n=1}^M k_{Fn}^2 = 2\pi n_0 d, \quad (13c)$$

where  $M$  is the number of occupied subbands and  $n_0$  is the density of conduction in the film. The electron density of states (per unit volume) is easily found to be

$$\frac{dn}{dE} = \frac{Mm}{\pi\hbar^2 d}. \quad (13d)$$

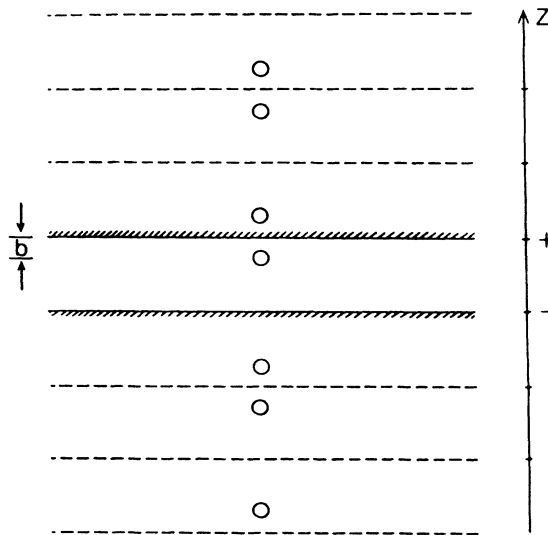


FIG. 1. Schematic diagram of a thin film of thickness  $d$ , an impurity inside the thin film and an array of image potentials.

In this section, we first derive an expression for the scattering state  $\psi_{n\mathbf{k}}^{(\pm)}$  in the confined thin film and then, following the method in Sec. II, we calculate the local potential arising from impurities in the film, the wind force on impurities, and the additional resistivity due to these impurities. Numerical examples are given also, in this section, for the  $d$  dependence of the surface resistivity of the thin film. A random distribution of impurities located near the surface of the film is used as a microscopic model for the surface roughness that leads to surface resistivity.

### A. Quantum-mechanical scattering problem

The scattering of a plane wave by the image-potential array is readily determined by standard techniques in low-energy electron diffraction (LEED) theory.<sup>33</sup> Steps to obtain  $\psi_{n\mathbf{k}}^{(\pm)}$  are outlined in this section. We first consider the incident wave

$$\phi_{\text{inc}} = e^{i\mathbf{K}_n^{(\pm)} \cdot \mathbf{r}}. \quad (14)$$

Since the image-potential is spherically symmetric, it is convenient to expand the wave in spherical harmonics. The expansion of the incident wave  $\phi_{\text{inc}}$  with respect to  $\mathbf{R}_{j\nu}$  is given by

$$\phi_{\text{inc}} = \sum_{l,m} a_{lm}^0(j,\nu) j_l(K|\mathbf{r} - \mathbf{R}_{j\nu}|) Y_{lm}(\hat{\Omega}(\mathbf{r} - \mathbf{R}_{j\nu})), \quad (15)$$

where

$$a_{lm}^0(j,\nu) = 4\pi(\pm i)^n i^{n+l} Y_{lm}^*(\hat{\mathbf{K}}_n^{(\pm)}) e^{\pm i n \nu b/d}, \quad (16)$$

and the  $(\pm)$  sign corresponds to  $\mathbf{K}_n^{(\pm)}$  of the incident wave. Since  $a_{lm}^0(j,\nu)$  is independent of  $j$ , then from symmetry arguments, we deduce that after multiple scattering between the potentials, the renormalized incident amplitude  $a_{lm}(j,\nu)$  is also independent of  $j$ . To simplify notation, we define  $a_{lm}(j,\nu) \equiv a_{lm}(\nu)$ . The following self-consistency condition is readily derived:<sup>34</sup>

$$a_{lm}(\nu) = a_{lm}^{(0)}(\nu) + i \sum_{j',\nu',l',m'} a_{l'm'}(\nu') e^{i\delta_{l'}} \sin\delta_{l'} \times G_{l'm',lm}(b(\nu - \nu')\hat{\mathbf{z}} - 2j'd\hat{\mathbf{z}}), \quad (17)$$

where the term which corresponds to  $j'=0$  and  $\nu=\nu'$  is not included in the summation.  $\delta_l$  is the impurity scattering phase shift, and  $G_{l'm',lm}(\mathbf{x})$  is defined by<sup>35</sup>

$$G_{l'm',lm}(\mathbf{x}) = \sum_{l''m''} 4\pi(i)^{(l'-l-l'')(-1)^{m+m''}} \times h_{l''}^{(1)}(K|\mathbf{x}|) Y_{l'',-m''}(\hat{\Omega}(\mathbf{x})) \times \int Y_{l'm'}(\hat{\Omega}) Y_{l''m''}(\hat{\Omega}) Y_{l,-m}(\hat{\Omega}) d\Omega,$$

where  $h_l^{(1)}$  is the spherical Hankel function of the first kind.<sup>36</sup> The second term on the right-hand side of Eq. (17) is the wave incident on one image potential due to the scattered wave from all other image potentials.

To obtain an analytic expression, we further simplify the model by restricting the scatterer to be a purely  $s$ -

wave scatterer. The matrix equation (17) then becomes a scalar equation for  $a_{00}(\nu)$ . We rename  $a_{00}(\nu)$  as  $a(\nu)$ . It can be shown that  $G_{00,00}(\mathbf{x})$  equals  $h_0^{(1)}(Kx)$ . The  $a(\nu)$  can be easily determined from the simplified Eq. (17). The total scattered wave is given by

$$\phi_{\text{sca}} = \frac{\sin\delta_0 e^{i\delta_0}}{\sqrt{4\pi}} \sum_{\nu} a(\nu) \sum_j \frac{e^{iK|\mathbf{r}-\mathbf{R}_{j\nu}|}}{K|\mathbf{r}-\mathbf{R}_{j\nu}|}, \quad (18)$$

where

$$\begin{pmatrix} a(1) \\ a(-1) \end{pmatrix} = \frac{1}{\Delta} \begin{pmatrix} 1-X(1,1) & X(1,-1) \\ X(1,-1) & 1-X(1,1) \end{pmatrix} \begin{pmatrix} a^0(1) \\ a^0(-1) \end{pmatrix}, \quad (19a)$$

and

$$\Delta = [1-X(1,1)]^2 - [X(1,-1)]^2. \quad (19b)$$

In Eq. (19),  $X(1,1) = \sin\delta_0 e^{i\delta_0} A_0$  and  $X(1,-1) = \sin\delta_0 e^{i\delta_0} B_0$ , where

$$A_0 = (\alpha\pi)^{-1} \sum_{j=1}^{\infty} \frac{\exp(2\pi i\alpha j)}{j}, \quad (20a)$$

and

$$B_0 = (2\pi\alpha)^{-1} \sum_{j=-\infty}^{\infty} \frac{\exp(2\pi i\alpha |j-b/d|)}{|j-b/d|} \quad (20b)$$

with  $K_F = \alpha\pi/d$ . Since only electrons around the Fermi surface are involved in the scattering, we take  $K$  to be  $K_F$ .

It is more convenient to convert the sum over unit cells in Eq. (18) into sum over the subband index. The conversion is done by applying the Poisson sum formula,<sup>37</sup> which is stated as follows: An infinite sum,  $\sum_{m=-\infty}^{\infty} f(2\pi m)$ , equals another infinite sum,  $(1/2\pi) \sum_{n=-\infty}^{\infty} F(n)$ , where  $F(n) = \int_{-\infty}^{\infty} f(\tau) e^{-in\tau} d\tau$ . The total scattered wave which corresponds to the incident wave  $e^{i\mathbf{K}_n^{\pm}\cdot\mathbf{r}}$  is found to be

$$\begin{aligned} \phi_{\text{sca}}(\mathbf{r}) = & (\pm i)^n \frac{\pi}{K_F d} \left[ \frac{e^{-i\delta_0}}{\sin\delta_0} - A_0 + B_0 \right]^{-1} \\ & \times \left[ i \cos(n\pi b/d) H_0^{(1)}(K_F \rho) + 2i \cos(n\pi b/d) \sum_{n'=1}^{\infty} \cos(n'\pi b/d) \cos[(n'\pi/d)(z-d/2)] \right. \\ & \quad \times H_0^{(1)}(\rho[K_F^2 - (n'\pi/d)^2]^{1/2}) \\ & \quad \left. \mp 2 \sin(n\pi b/d) \sum_{n'=1}^{\infty} \sin(n'\pi b/d) \sin[(n'\pi/d)(z-d/2)] H_0^{(1)}(\rho[K_F^2 - (n'\pi/d)^2]^{1/2}) \right], \quad (21) \end{aligned}$$

where  $H_0^{(1)}$  is the Hankel function of the first kind.<sup>36</sup>

The scattered state  $\phi^{(+)}$  is equal to  $\phi_{\text{inc}} + \phi_{\text{sca}}$ . For an incident wave of the form in Eq. (12), which is the linear superposition of two plane waves, the scattered state  $\psi_{n\mathbf{k}}^{(+)}$  is obtained from Eqs. (12), (14), and (21) to give

$$\begin{aligned} \psi_{n\mathbf{k}}^{(+)}(\mathbf{r}) = & \psi_{n\mathbf{k}}^0(\mathbf{r}) + \sqrt{2/\Omega} \frac{2\pi i}{K_F d} \left[ \frac{e^{-i\delta_0}}{\sin\delta_0} - A_0 + B_0 \right]^{-1} \sin(n\pi b/d) \\ & \times \sum_{n'=1}^{\infty} (-1)^{n+n'} \sin(n'\pi b/d) \sin[(n'\pi/d)(z+d/2)] H_0^{(1)}(\rho[K_F^2 - (n'\pi/d)^2]^{1/2}). \quad (22) \end{aligned}$$

The second term of Eq. (22) is the scattered wave and, because of the rotational symmetry of the image potential array about the  $z$  axis, is independent of the azimuthal angle  $\phi$ , for the case of an  $s$ -wave scatterer. The infinite sum in Eq. (22) can be interpreted as the amplitude of the incoming state  $\psi_{n\mathbf{k}}^0$  being scattered into states of subband index  $n'$ . If the electrons occupy  $M$  subbands, then for  $n' > M$ , we have  $K_F^2 < (n'\pi/d)^2$  and the Hankel function  $H_0^{(1)}(\rho[K_F^2 - (n'\pi/d)^2]^{1/2})$  becomes  $(2/\pi i) K_0(\rho[(n'\pi/d)^2 - K_F^2]^{1/2})$ , which is an exponentially decaying function for large argument. In general, the Fermi surface is not extremely close to a subband bottom, where the subband energy is  $(\hbar^2/2m)(n'\pi/d)^2$ . Hence the contribution from all  $n' > M$  terms in the infinite sum of Eq. (22) is small when  $\rho > d$  in the quantum-

mechanical asymptotic region. The closer the observation region is to the scatterer, the more of these evanescent waves are needed in the infinite sum for the scattered state. These evanescent waves can be interpreted as virtual transition processes that do not conserve energy. The quantum-mechanical asymptotic form of the scattered state  $\psi_{n\mathbf{k}}^{(+)}$  obtained from Eq. (22) is given by

$$\begin{aligned} \psi_{n\mathbf{k}}^{(+)}(\mathbf{r}) \simeq & \sqrt{2/\Omega} \sin[(n\pi/d)(z+d/2)] e^{ik\rho} \\ & + \sqrt{2/\Omega} \rho \sum_{n'=1}^M f_{nn'} e^{ik_{Fn'}\rho} \sin[n'\pi/d(z+d/2)], \quad (23) \end{aligned}$$

where

$$f_{nn'} = \frac{2}{K_F d} \left[ \frac{e^{-i\delta_0}}{\sin\delta_0} - A_0 + B_0 \right]^{-1} \left[ \frac{2\pi i}{k_{Fn'}} \right]^{1/2} \times \sin(n\pi b/d) \sin(n'\pi b/d) (-1)^{n+n'}. \quad (24)$$

We remark that the denominator of Eq. (24) involves  $A_0$  and  $B_0$ , which are sums over the positions of all image potentials [see Eq. (20)]. Thus this denominator has included the effects of all possible multiple scattering between these image potentials. Using the expression for  $\psi_{nk}^{(+)}$ , we apply the general method outlined in Sec. II to calculate the resistivity of thin metal films in the following subsections.

### B. Near-field potential and wind force

As discussed in Sec. I, the local potential setup near a scatterer in the region  $\rho < l$  is determined predominately by quantum-mechanical scattering occurring in the same region. In this subsection, we consider a current passing through a thin metal film and find the local potential in the vicinity of a scatterer as well as the electron wind force on the scatterer. The incident electron distribution is taken to be a shifted Fermi circle, for each occupied subband  $n$ , given by

$$g_{nk}^0 = -\tau e \mathbf{v}_k \cdot \hat{\mathcal{E}}_0 \delta(\epsilon_{nk} - E_F), \quad (25)$$

where  $\epsilon_{nk} = (\hbar^2/2m)[k^2 + (n\pi/d)^2]$  and the electric field  $\hat{\mathcal{E}}_0$  lies in the  $(x, y)$  plane. This distribution has the correct bulk limit in which case the quantized  $n\pi/d$  becomes a quasicontinuous wave vector  $k_z$ .

The electron density due to the electron current (or "electron wind") is given by the appropriate extension of Eq. (2), namely,  $\delta n_w(\mathbf{r}) = \sum_{n,k} g_{nk}^0 |\psi_{nk}^{(+)}(\mathbf{r})|^2$ . The quantum-mechanical asymptotic form of  $\psi_{nk}^{(+)}$  in Eq. (23) and the expression for  $g_{nk}^0$  in Eq. (25) are used to calculate  $\delta n_w(\mathbf{r})$ . After averaging over the film thickness, the electron density  $\delta n_w(\mathbf{r})$  becomes  $\delta n_w(\rho)$ . Introducing the self-consistent Thomas-Fermi screening condition of Eq. (3) with Eq. (13d), we find that the resulting local electrostatic potential near a scatterer has the form

$$\delta\Phi(\rho) = -p_{QM} \frac{\cos\phi}{\rho}. \quad (26a)$$

where  $\cos\phi = \hat{\rho} \cdot \hat{\mathcal{E}}_0$ . Here,  $\delta\Phi(\rho)$  is in the form of a two-dimensional dipole field, with the effective 2D dipole moment given by

$$p_{QM} = \frac{4\tau \mathcal{E}_0 \hbar}{md} \frac{\sum_{n=1}^M \sin^2(n\pi b/d)}{M} \times \text{Im} \left[ K_F^{-1} \left[ \frac{e^{-i\delta_0}}{\sin\delta_0} - A_0 + B_0 \right]^{-1} \right]. \quad (26b)$$

The subscript QM is a reminder that we are in the quantum-mechanical, or near-field, regime, where  $\rho < l$ .

We next find the electron wind force on the scatterer. The scattered current density is obtained from the ap-

propriately modified form of Eq. (5), namely,

$$J_\rho(z) = \frac{A}{2\pi^2} \sum_n \int d^2 k g_{nk}^0 \frac{\hbar}{m} \text{Re} \left[ \frac{1}{i} \psi_{nk}^{(+)*}(\mathbf{r}) \frac{\partial}{\partial \rho} \psi_{nk}^{(+)}(\mathbf{r}) - \frac{1}{i} \psi_{nk}^{0*}(\mathbf{r}) \frac{\partial}{\partial \rho} \psi_{nk}^0(\mathbf{r}) \right]. \quad (27)$$

$J_\rho(z)$  can be evaluated by substituting Eq. (23) into Eq. (27), and after the result is averaged over film thickness, the averaged scattered current density becomes

$$J_\rho = \frac{-\tau e \mathcal{E}_0}{md} \frac{\hat{\rho} \cdot \hat{\mathcal{E}}_0}{\rho} \sum_{n=1}^M \left[ \frac{2k_{Fn}^3}{\pi^3} \right]^{1/2} \text{Re}(f_{nn} e^{i\pi/4}). \quad (28)$$

We note that the sum in Eq. (28) corresponds to summing over the scattered radial current density in each occupied subband. The wind force on the scatterer along  $-\hat{\mathcal{E}}_0$  is related to  $J_\rho$  through the multiply occupied subband version of Eq. (4), with  $N=1$  in the present case. The wind force on a scatterer is found to be

$$F_w = \frac{4\tau e \mathcal{E}_0 \hbar}{md} \text{Im} \left[ K_F^{-1} \left[ \frac{e^{-i\delta_0}}{\sin\delta_0} - A_0 + B_0 \right]^{-1} \right] \times \sum_{n=1}^M k_{Fn}^2 \sin^2(n\pi b/d), \quad (29)$$

where we have substituted Eq. (24) for  $f_{nn}$  in Eq. (28). We notice that  $p_{QM}$  and  $F_w$  can be related to one another by comparing Eqs. (26b) and (29). The relation is particularly simple for the case of one occupied subband (i.e.,  $M=1$  case), which yields

$$F_w = e k_{F1}^2 p_{QM} \quad (30)$$

This relation is consistent with our previous results for a 2D electron gas.<sup>6</sup>

### C. Far-field potential and resistivity

The potential set up by a scatterer in the far-field region  $\rho > l$  is determined by both the quantum-mechanical scattering and the incoherent background scattering. Since the quantum-mechanical scattering occurs only within a region of size much smaller than  $l$  around the scatterer, we can separate the problem into two parts. The first part is to define a source term that includes the quantum-mechanical scattering effects, and the second part is to solve the Boltzmann equation with the source term. This approach was outlined in Sec. II.

The Boltzmann equation for electrons in a thin film is written as

$$\mathbf{v}_k \cdot \nabla_\rho g_{nk}(\rho) + e \mathcal{E}_0 \cdot \mathbf{v}_k \delta(\epsilon_{nk} - E_F) = \sum_{n',k'} W_{n',k',nk} g_{n',k'}(\rho) - \sum_{n',k'} W_{nk,n',k'} g_{nk}(\rho) + S_{nk}(\rho), \quad (31)$$

where

$$W_{n'\mathbf{k}',n\mathbf{k}} = (2\pi/\hbar)W_0\delta(\epsilon_{n'\mathbf{k}'} - \epsilon_{n\mathbf{k}})$$

is the transition rate from state  $|n', \mathbf{k}'\rangle$  to state  $|n, \mathbf{k}\rangle$  due to background scattering in the thin film, and  $W_0$  depends only on the energy of the electrons, which, in this case, is the Fermi energy  $E_F$ . The form of the transition rate is chosen such that it is isotropic on the  $k_x k_y$  plane and is also independent of the subband index. This assumed type of background scattering will become isotropic scattering in the bulk limit, for large  $d$ . In Eq. (31), the source term  $S_{n\mathbf{k}}(\boldsymbol{\rho})$  and the dynamic distribution function  $g_{n\mathbf{k}}(\boldsymbol{\rho})$  represent quantities that have been averaged over the film thickness. Since all particles involved have energies around  $E_F$ , the source term  $S_{n\mathbf{k}}(\boldsymbol{\rho})$  for a scatterer can be written in the following form

$$S_{n\mathbf{k}}(\boldsymbol{\rho}) = S(n, \hat{\mathbf{k}})\delta(\boldsymbol{\rho})\delta(\epsilon_{n\mathbf{k}} - E_F), \quad (32)$$

where the scatterer is located at  $\boldsymbol{\rho} = \mathbf{0}$ . It is also convenient to express  $g_{n\mathbf{k}}$  in the form

$$g_{n\mathbf{k}}(\boldsymbol{\rho}) = g_{n\mathbf{k}}^0 + G(n, \hat{\mathbf{k}}; \boldsymbol{\rho})\delta(\epsilon_{n\mathbf{k}} - E_F). \quad (33)$$

Using Eqs. (32), (33), and the form of  $W_{n'\mathbf{k}',n\mathbf{k}}$  in the collision integral, we can simplify the Boltzmann equation (31) to

$$\mathbf{v}_{\mathbf{k}} \cdot \nabla_{\boldsymbol{\rho}} G(n, \hat{\mathbf{k}}; \boldsymbol{\rho}) = \frac{1}{\tau} [\overline{G(\boldsymbol{\rho})} - G(n, \hat{\mathbf{k}}; \boldsymbol{\rho})] + S(n, \hat{\mathbf{k}})\delta(\hat{\boldsymbol{\rho}}). \quad (34a)$$

Here,  $\tau = AmMW_0/\hbar^3$  is the relaxation time, and

$$\overline{G(\boldsymbol{\rho})} = \frac{1}{2\pi M} \sum_{n'} \int d\phi_{\hat{\mathbf{k}}} G(n', \hat{\mathbf{k}}'; \boldsymbol{\rho}), \quad (34b)$$

is the local average to which the electrons relax.

The expression for the source term  $S(n, \hat{\mathbf{k}})$  is obtained, following an argument similar to that in Sec. II. The rate of particles being emitted by the source into subband  $n$  and solid angle  $\Delta\Omega_{\hat{\mathbf{k}}}$  is given by

$$\frac{2d}{(2\pi)^2} \int dk k \int d\boldsymbol{\rho} S_{n\mathbf{k}}(\boldsymbol{\rho}) \Delta\Omega_{\hat{\mathbf{k}}}.$$

However, the rate can also be expressed in terms of the radial scattered current density in subband  $n$  from Eq. (28). Upon equating the two rate expressions, we deduce that

$$S(n, \hat{\mathbf{k}}) = -\frac{\tau e \mathcal{E}_0}{d} \left[ \frac{\hbar}{m} \right]^2 \hat{\mathbf{k}} \cdot \hat{\mathcal{E}}_0 (8\pi k_{Fn}^3)^{1/2} \text{Re}(f_{nn} e^{i\pi/4}). \quad (35)$$

To solve the Boltzmann equation, we first Fourier transform Eq. (34a), using the convention

$$f(\mathbf{q}) = \int d\boldsymbol{\rho} e^{-i\mathbf{q}\cdot\boldsymbol{\rho}} f(\boldsymbol{\rho}). \quad (36)$$

After some algebra, we arrive at the expression of  $\overline{G(\mathbf{q})}$

$$\begin{aligned} \overline{G(\mathbf{q})} = & -i \frac{\hat{\mathbf{q}} \cdot \hat{\mathcal{E}}_0}{q} \frac{8\pi\tau e \mathcal{E}_0 \hbar}{md^2} \text{Im} \left[ K_F^{-1} \left[ \frac{e^{-i\delta_0}}{\sin\delta_0} - A_0 + B_0 \right]^{-1} \right] \\ & \times \frac{\sum_{n=1}^M \sin^2(n\pi b/d) I_n(\mathbf{q})}{\sum_{n=1}^M I_n(\mathbf{q})}, \end{aligned} \quad (37)$$

where the integral  $I_n(\mathbf{q})$  is defined as

$$\begin{aligned} I_n(\mathbf{q}) &= \frac{1}{2\pi M} \int d\phi_{\hat{\mathbf{k}}} \frac{l_n^2 q^2 (\hat{\mathbf{k}} \cdot \hat{\mathbf{q}})^2}{1 + l_n^2 q^2 (\hat{\mathbf{k}} \cdot \hat{\mathbf{q}})^2} \\ &= \frac{1}{M} \left[ 1 - \frac{1}{(1 + l_n^2 q^2)^{1/2}} \right]. \end{aligned} \quad (38)$$

Here  $l_n = \hbar k_{Fn} \tau / m$  is the mean free path for electrons in subband  $n$ . The limiting forms of  $I_n(\mathbf{q})$  are

$$I_n(\mathbf{q}) \simeq \begin{cases} l_n^2 q^2 / 2M & \text{for } l_n q \ll 1, \\ 1/M & \text{for } l_n q \gg 1. \end{cases} \quad (39)$$

It is now straightforward to find the perturbed electron density, given by

$$\begin{aligned} \delta n_w(\boldsymbol{\rho}) &= \frac{2}{(2\pi)^4} \sum_{n=1}^M \int d\mathbf{k} \int d\mathbf{q} e^{i\mathbf{q}\cdot\boldsymbol{\rho}} G(n, \hat{\mathbf{k}}; \mathbf{q}) \delta(\epsilon_{n\mathbf{k}} - E_F) \\ &= \frac{Mm}{4\pi^3 \hbar^2} \int d\mathbf{q} e^{i\mathbf{q}\cdot\boldsymbol{\rho}} \overline{G(\mathbf{q})}. \end{aligned} \quad (40)$$

We apply the neutralization condition, as given in Eq. (3), to find the local electrostatic potential  $\delta\Phi(\boldsymbol{\rho})$  set up by the scatterer. The result is

$$\delta\Phi(\boldsymbol{\rho}) = -\frac{d}{4\pi^2 e} \int d\mathbf{q} e^{i\mathbf{q}\cdot\boldsymbol{\rho}} \overline{G(\mathbf{q})}, \quad (41)$$

where we have used Eq. (13d).

In the case when  $\rho \gg l_n$ , for all occupied subbands  $n$ ,<sup>38</sup> the integral in Eq. (41) is determined by the region  $l_n q \ll 1$ . Therefore, using the small- $q$  ( $l_n q \ll 1$ ) approximation of  $I_n(\mathbf{q})$ , given by Eq. (39), and substituting Eqs. (37) into (41), we find:

$$\delta\Phi(\boldsymbol{\rho}) = -p_{\text{RRD}} \frac{\cos\phi}{\rho}, \quad (42)$$

where

$$\begin{aligned} p_{\text{RRD}} &= \frac{4\tau \mathcal{E}_0 \hbar}{md} \text{Im} \left[ K_F^{-1} \left[ \frac{e^{-i\delta_0}}{\sin\delta_0} - A_0 + B_0 \right]^{-1} \right] \\ &\quad \times \frac{\sum_{n=1}^M \sin^2(n\pi b/d) k_{Fn}^2}{\sum_{n=1}^M k_{Fn}^2}. \end{aligned} \quad (43)$$

Eq. (42) shows that after averaging over the film thickness, the long-range potential has the form of a 2D dipole field, with  $p_{\text{RRD}}$  being the 2D dipole moment.

We can also consider the small- $\rho$  limit, i.e.,  $\rho \ll l_n$  for all occupied subbands  $n$ , of Eq. (41). This limit is easily obtained by taking  $\tau$  large, so that the condition  $\rho \ll l_n$  is

satisfied for any finite  $\rho$ . Using Eqs. (37), (41), and the large- $l_n q$  limit of  $I_n(q)$  in Eq. (39), we get  $\delta\Phi(\rho) = -p_{QM} \cos\phi/\rho$ , which is identical to the local potential we obtain in Eq. (26a) using the full quantum mechanical approach. Hence, the local potential  $\delta\Phi(\rho)$  for arbitrary  $\rho$ , is given by

$$\begin{aligned} \delta\Phi(\rho) = & \frac{2\tau\mathcal{E}_0\hbar}{\pi md} \text{Im} \left[ K_F^{-1} \left[ \frac{e^{-i\delta_0}}{\sin\delta_0} - A_0 + B_0 \right]^{-1} \right] \\ & \times \int d\mathbf{q} e^{i\mathbf{q}\cdot\rho} \frac{i\hat{\mathbf{q}}\cdot\hat{\mathbf{e}}_0}{q} \\ & \times \frac{\sum_{n=1}^M \sin^2(n\pi b/d) \left[ 1 - \frac{1}{(1+I_n^2 q^2)^{1/2}} \right]}{\sum_{n=1}^M \left[ 1 - \frac{1}{(1+I_n^2 q^2)^{1/2}} \right]}. \end{aligned} \quad (44)$$

The resistivity due to the scatterer can be defined by applying two electrodes, one at the left-hand end and the other at the right-hand end of the thin film. Assuming that the left-to-right direction is  $\hat{x}$ , we allow these electrodes to extend over the entire cross section of the thin film, with the cross-sectional area parallel to the  $yz$  plane. The average potential difference between these two electrodes is given by  $2\pi p_{RRD}/L_y$ , where  $L_x$  is the length and  $L_y$  is the width of the film. We have used the long-range potential in Eq. (41) and have assumed  $L_x < L_y$ . The average electric field  $\delta\mathcal{E}$  is equal to  $2\pi p_{RRD}/L_x L_y$ . The additional resistivity for one scatterer is  $\delta\mathcal{E}/J_0$ , where  $J_0 = n_0 e^2 \tau \mathcal{E}_0/m$ , and  $n_0$  is the electron density in the film. Assuming a dilute density of  $n_i$  independent impurities per unit area of the film, the additional resistivity due to these impurities is given by

$$\begin{aligned} \Delta\rho = & \frac{\hbar}{e^2} \frac{4n_i}{n_0^2 d^2} \text{Im} \left[ K_F^{-1} \left[ \frac{e^{-i\delta_0}}{\sin\delta_0} - A_0 + B_0 \right]^{-1} \right] \\ & \times \sum_{n=1}^M k_{Fn}^2 \sin^2 \left[ \frac{n\pi b}{d} \right], \end{aligned} \quad (45)$$

where we have used Eq. (13c) in Eq. (43).

The expression for  $\Delta\rho$  in Eq. (45) is shown to be valid even for the thick film regime ( $d > l$ ) in Appendix B. Therefore, in this regime we have

$$\begin{aligned} \frac{\Delta\rho}{\rho_\infty} = & 4\pi \frac{n_i}{k_F^2} \frac{l}{d} \text{Im} \left[ \left[ \frac{e^{-i\delta_0}}{\sin\delta_0} - A_0 + B_0 \right]^{-1} \right] \\ & \times \left[ 1 - \frac{3j_1(2k_F b)}{2k_F b} \right], \end{aligned} \quad (46)$$

where  $\rho_\infty$  is the bulk resistivity and  $k_F$  is the bulk Fermi wave vector.

The Fuchs-Sondheimer<sup>23,24</sup> theory gives the following expression for  $\Delta\rho/\rho_\infty$  of a film of finite thickness:

$$\frac{\Delta\rho}{\rho_\infty} = 1 - \frac{3}{2\kappa} \int_0^1 du \frac{(u-u^3)(1-p)[1-\exp(-\kappa/u)]}{1-p\exp(-\kappa/u)}, \quad (47a)$$

where  $\kappa = d/l$ . In the thick-film regime this yields

$$\frac{\Delta\rho}{\rho_\infty} = \frac{3}{8}(1-p)\frac{l}{d}. \quad (47b)$$

Both Eqs. (46) and (47b) are in agreement as far as their linear dependence on  $l/d$  is concerned.

We have derived the electron wind force [Eq. (29)], the local potential [Eq. (44)], the small- $\rho$  limit of the local potential [Eq. (26a)], the long-range limit of the local potential [Eq. (42)], and the resistivity due to a layer of scatterers in thin metal film with flat surfaces [Eq. (45)]. We now look at the relationship between these quantities for the one-scatterer case. The resistivity of one scatterer, which we denote by  $\delta\rho$ , can be obtained from Eq. (45) by setting  $n_i$  equal to  $1/L_x L_y$ . Comparison of Eqs. (43) and (45) yields the relation between  $p_{RRD}$  and  $\delta\rho$ , which is

$$\delta\rho = \frac{2\pi p_{RRD}}{J_0 L_x L_y}. \quad (48)$$

We note that  $p_{RRD}$  is the effective RRD, which is a 2D dipole in film geometry. The relation between wind force and resistivity is obtained by comparing Eqs. (29) and (45), which yields

$$\delta\rho = \frac{1}{n_0 e} \frac{F_w}{J_0 L_x L_y d}. \quad (49)$$

The close relationship between  $\delta\rho$ ,  $p_{RRD}$ , and  $F_w$  is clearly demonstrated by Eqs. (48) and (49). We remark that the relation (49) can be cast into the form of the well-known wind-force expression for dilute impurities in a 3D electron gas, namely,<sup>11</sup>

$$F_w = -\frac{\Delta\rho}{\rho_0 N_i} n_0 e \mathcal{E}_0, \quad (50)$$

where  $N_i$  is the number of impurities per unit volume and  $\rho_0$  is the background resistivity. Equation (50) follows upon substituting  $J_0 = \mathcal{E}_0/\rho_0$  and  $\delta\rho = \Delta\rho/N_i L_x L_y d$  in Eq. (49).

#### D. Numerical results

For numerical examples, we consider the resistivity due to scatterers located near the film surface, and plot the resistivity against film thickness, using Eq. (45). As this arrangement of scatterers can be used as a microscopic model for surface roughness, the numerical results give the resistivity due to surface roughness in a thin film. We choose  $b = 3\pi/8k_F$  so that the scatterers are on the jellium edge in the case of thick films. For the thin-film case, even though the jellium edge is not so sharply defined, we still keep the same  $b$  value since it is small enough to serve the purpose of a reasonable model for surface roughness.

In Fig. 2, we present the plot of the normalized surface resistivity  $\Delta\rho/\rho_\infty$  versus the logarithm of the film thick-

ness  $d$  for representative choices of parameters  $k_F$ ,  $l$ ,  $\delta_0$ , and  $n_i$ . The mean free path  $l$  is introduced into the infinite sums  $A_0$  and  $B_0$  in Eq. (45) by giving  $K_F$  an imaginary part equal to  $1/l$ . (This gives rise to the usual damping factor in the electron propagator.) The electron density  $n_0$  is fixed at the bulk value for the material of interest, which is parametrized in terms of the bulk Fermi

wave vector  $k_F$  where  $k_F = (3\pi^2 n_0)^{1/3}$ . We choose  $k_F = 0.415$  a.u., which corresponds to the electron density for  $\text{CoSi}_2$ . (Epitaxial single-crystal films of metalliclike  $\text{CoSi}_2$  films grown on Si have recently been prepared.<sup>22</sup>) We also performed calculations for a Sn film ( $k_F = 0.8642$  a.u.), and found that the essential features of the thickness dependence of  $\Delta\rho/\rho_0$  are the same as for a  $\text{CoSi}_2$

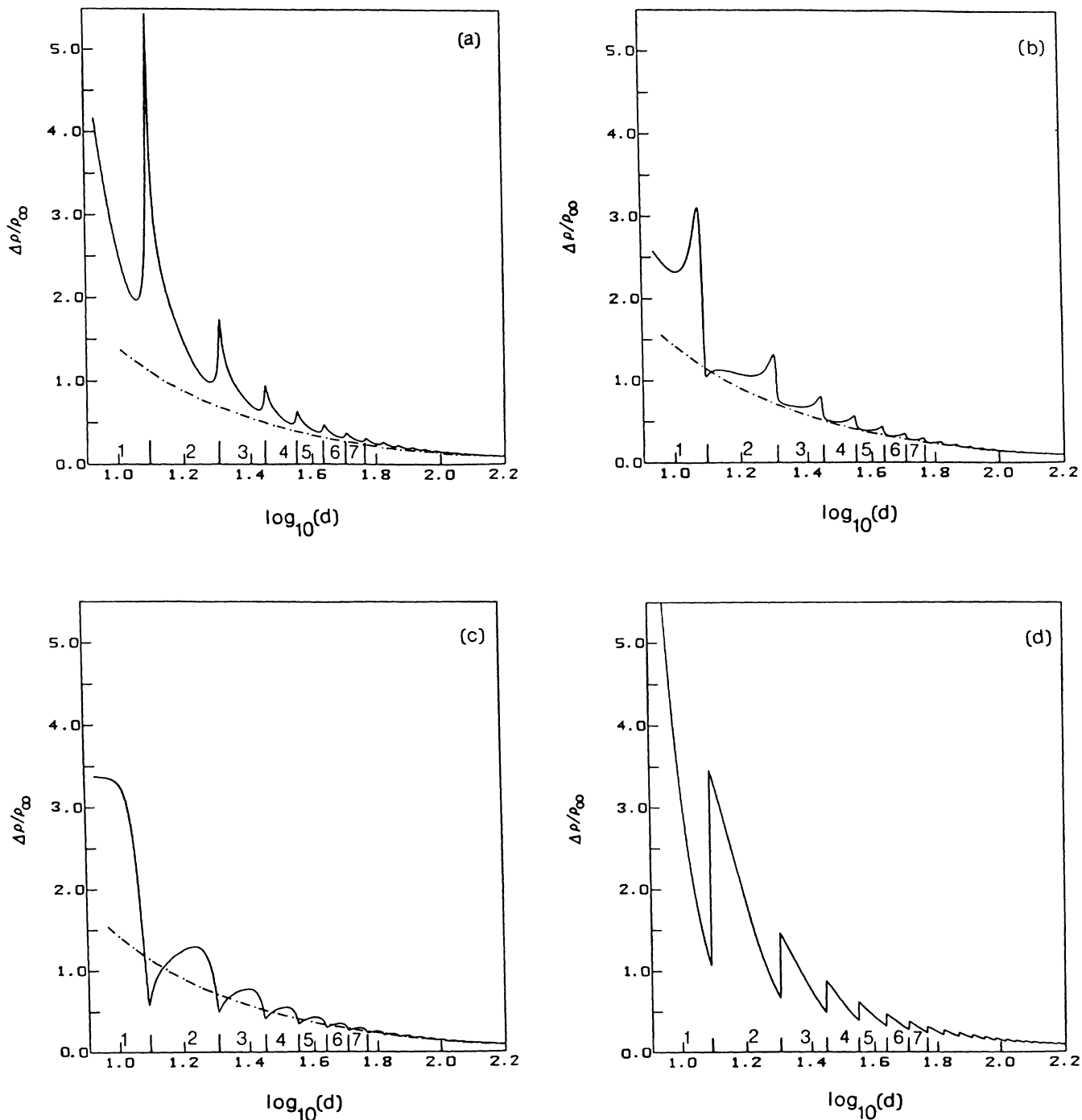


FIG. 2. Resistivity ( $\Delta\rho/\rho_\infty$ ) due to impurities in a thin film is plotted as a function of  $\log_{10}(d)$ . The physical parameters are  $k_F = 0.415$  a.u.,  $l = 200$  Å, and (a)  $\delta = 30^\circ$ ,  $n_i = 0.412 \times 10^{-2}$  a.u.; (b)  $\delta = 60^\circ$ ,  $n_i = 0.918 \times 10^{-3}$  a.u.; (c)  $\delta = 90^\circ$ ,  $n_i = 0.926 \times 10^{-3}$  a.u. The Born-approximation result is shown in (d). The number of occupied subbands is indicated up to  $M = 7$ . The parameters are chosen to give the asymptotic Fuchs-Sondheimer result for  $p = 0.9$ . The latter is indicated by dot-dashed curves in (a), (b), and (c).

film. The bulk mean free path  $l$  is chosen to be 200 Å. The phase shift  $\delta_0$  is chosen to be 30°, 60°, and 90°, respectively, in (a), (b), and (c) of Fig. 2. For easier comparison, all the graphs are scaled so that they approach the Fuchs-Sondheimer theory, for  $p=0.9$ , in the thick-film region. [This requires  $n_i$  to depend on the choice of phase shift. In Fig. 2, the  $n_i$  values are  $0.412 \times 10^{-2}$ ,  $0.918 \times 10^{-3}$ , and  $0.926 \times 10^{-3}$ , a.u. in (a), (b), and (c), respectively. Since  $\Delta\rho/\rho_\infty$  is proportional to  $n_i$ , the values of  $\Delta\rho/\rho_\infty$  for any  $n_i$  can be obtained for each  $\delta_0$  by a simple scaling.] In Fig. 2(d) we show the result in the weak-scattering limit, i.e., in the Born approximation. The latter is obtained by expanding expression (45) to second order in  $\delta_0$ . This results in the replacement of

$$\text{Im} \left[ K_F^{-1} \left[ \frac{e^{-i\delta_0}}{\sin\delta_0} - A_0 + B_0 \right]^{-1} \right]$$

by

$$\frac{2\pi\delta_0^2}{K_F^2 d} \sum_{\nu=1}^M \sin^2(\nu\pi b/d) \quad (51)$$

in Eq. (45).

The surface resistivity graphs in Fig. 2 exhibit a series of peaks, with larger height in the region of smaller  $d$ . The overall trend of the graphs is that the resistivity increases as the thickness decreases. The resistivity is increasing faster than the asymptotic Fuchs-Sondheimer result [given by Eq. (47b)], which is shown by the dot-dashed curve in the figures. We remark that the asymptotic Fuchs-Sondheimer result is greater than the exact Fuchs-Sondheimer result [given by Eq. (47a)] in the small- $d$  regime.<sup>21</sup>

The resistivity changes most rapidly in the immediate vicinity of the  $d$  values where the Fermi level lies at a subband bottom. (The location of these particular  $d$  values and the number of occupied subbands are indicated up to  $M=7$  in Fig. 2.) As  $d$  increases,  $E_F$  changes continuously [ $E_F$  is determined self-consistently from Eqs. 13(b) and 13(c) by requiring that the electron density in the film is kept fixed at  $n_0$ ]. However,  $dn/dE$ , given by Eq. 13(d), undergoes a discontinuous upward jump as  $d$  increases through the critical  $d$  values, since  $M$  increases by unity at these  $d$  values. The resistivity also tends to exhibit a sudden increase at these  $d$  values because a new channel for scattering appears. This effect is seen clearly in the Born-approximation curve, Fig. 2(d), the precise form of which depends upon matrix element effects which can be traced to the explicit  $b$  dependence of the terms in Eq. (45) and expression (51).

In addition to the aforementioned density-of-states and matrix-element effects, there is another effect due to multiple scattering between the impurity and the surfaces. This effect is contained in the factor containing the sums  $A_0$  and  $B_0$  in Eq. (45), and appears when that factor is evaluated beyond the lowest-order term (51). The extent to which Figs. 2(a)–2(c) deviate from Fig. 2(d) is a manifestation of the multiple-scattering effect. As expected, the deviation is most pronounced for the strongest scatterer, i.e., in Fig. 2(c). As is apparent from Fig. 2(c),

the multiple-scattering effect tends to depress the resistivity in the immediate vicinity of the onset of a new subband. We remark that if the mean free path were effectively infinite, the  $\Delta\rho/\rho_\infty$  curves would exhibit extremely narrow downward spikes extending all the way to zero at the critical  $d$  values marking the onset of a new subband. These downward spikes do not persist unless  $l$  is very large, however, and are essentially washed away for  $l=200$  Å. The distinct dips in Fig. 2(c) are a remnant of this multiple-scattering transparency effect.

#### IV. DISCUSSION

The RRD is the source of the long-range microscopic field associated with electron scattering by impurities and interfaces in metallic microstructures. For a single impurity in bulk, the residual resistivity  $\delta\rho$  and the electromigration wind force  $F_w$  are directly related to the RRD strength, which thus provides a link between  $\delta\rho$  and  $F_w$ . Using the local-field method, we have generalized the above relationships to systems consisting of impurities in thin metal films. The results are given in Eqs. (48)–(50). For the case of an impurity in a thin metal film, the near-field potential and the far-field potential are dipolar and are characterized by dipolar strength  $p_{QM}$  and  $p_{RRD}$  respectively, as given in Eqs. (26b) and (43). The near-field region does not include the immediate surroundings of the impurities because we have used the asymptotic scattering state expression in Eq. (23). The exact scattering state, given by Eq. (22), has evanescent wave components which, in general, can be neglected in the region where  $\rho > d$ . However, for thicker films ( $k_F d \gg 1$  and  $d > l$ ), Eq. (23) is shown in Appendix B to become the correct asymptotic scattering state for an impurity near the surface of a semi-infinite medium. Therefore, Eq. (23) is a good approximation to Eq. (22) when  $\rho > d$  in thin films and when  $k_F \rho > 1$  in thick films. In the immediate surroundings of the impurity, i.e., for even smaller  $\rho$ , the evanescent waves cannot be neglected, and Eq. (22) has to be used to calculate the electron density and the electrostatic potential in this region, following the local-field method.

The two dipolar strengths  $p_{QM}$  and  $p_{RRD}$  are equal only in the 2D limit, in which case there is one occupied subband. In general  $p_{QM}$  and  $p_{RRD}$  are different from one another. This is in contrast to the 3D case<sup>2,5</sup> and the pure 2D case,<sup>6</sup> where the dipole for the near field is the same as the dipole for the far field. The different values of  $p_{QM}$  and  $p_{RRD}$  are due to different values for the mean free path  $l_n$  in each subband, which causes the electrons in different subbands to scatter and pileup according to different length scales  $l_n$ . Indeed, if we let all  $l_n$  be the same in Eq. (44) for the local potential, we see that the near-field dipole would be the same as the far-field dipole and both would equal  $p_{QM}$ . We also point out that the field of the dipole in a thin film falls off more slowly with distance than the field of a 3D dipole. Therefore, the potential drop across an impurity is larger in a thin film than in bulk metal, assuming that the voltage probes are equivalently positioned in the two cases and that the dipole strengths are comparable. In Appendix B, we have

also shown that the resistivity expression in Eq. (45) is valid for all  $d$ .

We calculated the surface resistivity of a thin film by assuming a microscopic model in which surface roughness arises from a random distribution of impurities near the surface. When plotted against film thickness, the surface resistivity exhibits oscillatory features, which are related to discrete jumps in the density of states and to multiple scattering between an impurity and the film surfaces. In thicker films ( $d > l$ ), the variation of the surface resistivity with film thickness equals that of the Fuchs-Sondheimer results for an appropriate choice of  $p$ . In the thin film limit, the surface resistivity, as given by Eq. (45), deviates from, and is generally greater than, the Fuchs-Sondheimer result. For the parameters chosen here, the deviations are not so large as those found by Tešanović *et al.*<sup>30</sup> or, most recently, by Trivedi and Ashcroft.<sup>39</sup>

The local-field method focuses attention on microscopic charge distributions arising from scattered wave functions and on the resulting potential field that is self-consistently generated. In principle, this potential field can be measured by noninvasive probes at the surface of the sample. Calculations performed within the framework of the local-field method also give insight into the importance of sample geometry, impurity configuration, and electrode placement in a voltage measurement.

In applying the method it was necessary to specify the form of the nonequilibrium distribution  $g_k^0$  which is incident on an impurity scatterer group. For the case of a short microstructure placed between reservoirs,  $g_k^0$  can be regarded as established by the reservoirs. In that case, all multiple scattering processes within the microstructure are to be taken into account. This is the usual picture envisioned in application of the (multichannel) Landauer formula. For the case of a very long microstructure, such as the thin-film system considered in this work, where the film length is assumed to be very much larger than the background mean free path and the average distance between impurities, it is not practical to solve the complete multiple-scattering problem. Consequently, we assumed that well into the microstructure there exists a  $g_k^0$  that describes an incoherent beam of electrons incident on a typical scatterer group. We further assumed that  $g_k^0$  has the form of a shifted Fermi distribution corresponding to a current carrying state in the presence of uniform incoherent background scattering. These assumptions are certainly justifiable if the background resistivity,  $\rho_0$ , is much larger than the impurity resistivity  $\Delta\rho$ . Stated in a perhaps less restrictive way, our calculation scheme correctly determines the linear coefficient  $\alpha$  in the following expansion of the total resistivity in powers of the impurity density:

$$\rho = \rho_0 + \alpha n_i + O(n_i^2), \quad (52)$$

where  $\rho_0$  is finite (nonzero) and we envision  $n_i \rightarrow 0$ . Our  $\Delta\rho$  calculation would then be valid so long as we remain in the linear regime of Eq. (52). In the more general case, a better approximation scheme is to choose  $g_k^0$  as the solution of the conventional Boltzmann equation for random surface impurities in a medium characterized by

uniform background scattering. In this case, surface-impurity scattering and the background scattering would enter the Boltzmann equation in the usual way via ensemble-averaged translational probabilities in the collision integral. The resulting  $g_k^0$  solution could then be used in the calculations described in Secs. II and III for the microscopic charge distribution and local potential near an impurity. We have performed a resistivity calculation based upon such a model and have found that the corrections to the  $\Delta\rho/\rho_\infty$  curves of Fig. 2 are relatively minor.<sup>40</sup> We conclude that the approximation we have made in choosing  $g_k^0$  is acceptable here.

Further possible improvements are difficult to obtain within a conventional Boltzmann equation approach. However, within Landauer's picture a further correction, which is formally higher order in impurity concentration, can be considered. This is the so-called Lorentz correction,<sup>41</sup> which is a renormalization effect arising from current rerouting from one impurity to another. This causes the incident current upon an impurity to be larger than the average current in the medium, resulting in a larger RRD strength and larger  $\Delta\rho$ . Formally such corrections are of order  $n_i^2$ , and do not appear to significantly modify our numerical results, even for the larger  $n_i$ -values considered in Fig. 2.

The major limitation of the thin-film resistivity calculation is in the model itself rather than in the approximations made in obtaining Eq. (45). We have modeled the film as a free-electron gas confined between infinite barriers which define perfectly flat surfaces. The underlying crystal structure of the material as well as large-scale surface irregularities are lost in this jellium model. Only small-scale, surface-impurity scattering effects were treated, and this was done only for the case of  $s$  like scatterers. Despite these limitations, our results for the  $d$  dependence of  $\Delta\rho/\rho_\infty$  should be qualitatively valid, giving the same overall trend as would be obtained in a more realistic model. For example, long-range departures of the film surface from perfect flatness would, in the first approximation, be equivalent to averaging our  $\Delta\rho/\rho_\infty$  curves over a small window of  $d$  values. This would result in a slight smoothing of the curves, but the overall trend would remain.

Finally, we remark that we have not considered local-field contributions arising from the polarization of electrons brought in by the impurity in the presence of the electric field  $\mathcal{E}_0$ . Such effects enter the so-called "direct force" in electromigration theory,<sup>11-17,42</sup> and have been described by Landauer in terms of carrier density modulation.<sup>43</sup> Formally, such effects are of order  $1/(k_F l)$  times the electron-wind effects considered here, and thus can be neglected for free-electron-like metals.

#### ACKNOWLEDGMENT

This work was supported by the Rome Air Development Center, United States Air Force.

#### APPENDIX A: LOCAL FIELD METHOD FOR AN IMPURITY IN BULK

The bulk impurity is described by a spherically symmetric muffin-tin potential. For an incident plane wave

state  $\psi_{\mathbf{k}}^0$ , the scattering state  $\psi_{\mathbf{k}}^{(+)}$  in the quantum-mechanical asymptotic region ( $kr \gg 1$ ) is given by

$$\psi_{\mathbf{k}}^{(+)}(\mathbf{r}) = \frac{1}{\sqrt{\Omega}} \left[ e^{i\mathbf{k}\cdot\mathbf{r}} + \frac{f(\theta)}{r} e^{ikr} \right], \quad (\text{A1})$$

where

$$f(\theta) = \frac{1}{k} \sum_l (2l+1) P_l(\cos\theta) e^{i\delta_l} \sin\delta_l,$$

$P_l$  is the Legendre polynomial,  $\delta_l$  is the impurity scattering phase shift and  $\Omega$  is the volume of the bulk metal. We apply the local-field method outlined in Sec. II to calculate the far-field potential.

Using Eq. (5), we find the radial scattered particle current density:

$$J_r(\mathbf{r}) = \frac{3S_0 I_0}{4\pi} \frac{\hat{\mathbf{r}} \cdot \hat{\mathcal{E}}_0}{r^2} \hat{\mathbf{r}}, \quad (\text{A2})$$

where  $S_0 = \int d\Omega |f(\theta)|^2 (1 - \cos\theta)$  is the dynamic scattering cross section, and  $I_0 = e\tau k_F^3 \mathcal{E}_0 / 3\pi^2 m$  is the particle current density far from the impurity. The source term in the Boltzmann equation is obtained from Eq. (8). The result is

$$S(\hat{\mathbf{k}}) = \mathcal{S} \hat{\mathbf{k}} \cdot \hat{\mathcal{E}}_0, \quad (\text{A3})$$

where  $\mathcal{S} \equiv (3\pi^2 \hbar^2 / mk_F) S_0 I_0$ . After substituting Eqs. (7) and (9) into Eq. (6), the Boltzmann equation becomes

$$\mathbf{v}_{\mathbf{k}} \cdot \nabla_{\mathbf{r}} G(\hat{\mathbf{k}}, \mathbf{r}) = -\frac{1}{\tau} [G(\hat{\mathbf{k}}, \mathbf{r}) - \overline{G(\mathbf{r})}] + \mathcal{S} \hat{\mathbf{k}} \cdot \hat{\mathcal{E}}_0 \delta(\mathbf{r}), \quad (\text{A4})$$

where

$$\overline{G(\mathbf{r})} = \frac{1}{4\pi} \int d\Omega_{\hat{\mathbf{k}}} G(\hat{\mathbf{k}}, \mathbf{r}).$$

To solve the Boltzmann equation, we first Fourier transform (A4), using the convention

$$f(\mathbf{q}) = \int d\mathbf{r} e^{-i\mathbf{q}\cdot\mathbf{r}} f(\mathbf{r}). \quad (\text{A5})$$

After some algebraic manipulations, we obtain

$$\overline{G(\mathbf{g})} = \frac{\tau \mathcal{S}}{ilq} \hat{\mathbf{q}} \cdot \hat{\mathcal{E}}_0, \quad (\text{A6})$$

where  $l = \hbar k_F \tau / m$  is the mean free path.

The perturbed electron density  $\delta n_w(\mathbf{r})$  due to the current density is given by Eq. (10):

$$\begin{aligned} \delta n_w(\mathbf{r}) &= \frac{2}{(2\pi)^3} \int d\mathbf{k} \frac{1}{(2\pi i)^3} \int d\mathbf{q} e^{i\mathbf{q}\cdot\mathbf{r}} G(\hat{\mathbf{k}}, \mathbf{q}) \delta(\epsilon_{\mathbf{k}} - E_F) \\ &= \frac{mk_F}{8\pi^5 \hbar^2} \int d\mathbf{q} e^{i\mathbf{q}\cdot\mathbf{r}} \overline{G(\mathbf{q})} \\ &= \frac{mk_F}{8\pi^5 \hbar^2} \frac{\tau \mathcal{S}}{il} \int d\mathbf{q} e^{i\mathbf{q}\cdot\mathbf{r}} \frac{\hat{\mathbf{q}} \cdot \hat{\mathcal{E}}_0}{q}. \end{aligned} \quad (\text{A7})$$

Using the integral result

$$\int_0^\infty e^{ikx} x dx = -i\pi \delta'(k) - 1/k^2, \quad (\text{A8})$$

we calculate the integral in Eq. (A7):

$$\int d\mathbf{q} e^{i\mathbf{q}\cdot\mathbf{r}} \frac{\hat{\mathbf{q}} \cdot \hat{\mathcal{E}}_0}{q} = i2\pi^2 \frac{\hat{\mathbf{r}} \cdot \hat{\mathcal{E}}_0}{r^2}. \quad (\text{A9})$$

$\delta n_w$  can be obtained by substituting Eqs. (A9) into (A7). The far-field potential  $\delta\Phi(\mathbf{r})$  is then calculated, from Eq. (3), to give

$$\delta\Phi(\mathbf{r}) = -\frac{p \cos\theta}{r^2}, \quad (\text{A10})$$

where  $\cos\theta = \hat{\mathbf{r}} \cdot \hat{\mathcal{E}}_0$  and  $p \equiv 3\pi \hbar S_0 I_0 / 4k_F^2 e$  is the RRD moment. We have used the fact that the density of states in bulk is  $dn/dE = mk_F / (\pi \hbar)^2$ .

## APPENDIX B: RESISTIVITY OF THICK FILMS

We first show that, in the thick film limit ( $d > l$ ), the scattered state  $\psi_{n\mathbf{k}}^{(+)}$  in Eq. (23) becomes the scattered wave in the region  $k_F r \gg 1$  for the case of an impurity near the surface of a semi-infinite medium. Since  $d > l$ , only the  $j=0$  term in  $A_0$  and  $B_0$  is kept, and the scattered wave  $\psi_{n\mathbf{k}}^{(+)}$  becomes

$$\begin{aligned} \psi_{n\mathbf{k}}^{(+)}(\mathbf{r}) &= \sqrt{2/\Omega} (-1)^n \sin \left[ \frac{n\pi}{d} z \right] e^{i\mathbf{k}\cdot\mathbf{r}} + \sqrt{\pi i/\Omega} \frac{(-1)^n}{(r_{\parallel})^{1/2}} \frac{4}{k_F d} \left[ \frac{e^{-i\delta_0}}{\sin\delta_0} + i h_0^{(1)}(2k_F b) \right]^{-1} \\ &\quad \times \sin(k_1 b) \sum_{n'=1}^m \frac{1}{(k'_{\parallel})^{1/2}} \sin(k'_1 b) \sin(k'_1 z) e^{ik'_{\parallel} \rho}, \end{aligned} \quad (\text{B1})$$

where  $k_1 \equiv n\pi/d$ ,  $k'_1 \equiv n'\pi/d$ ,  $k'_{\parallel} \equiv (k_F^2 - k_1'^2)^{1/2}$ ,  $K_F = k_F$ ,  $r_{\parallel} \equiv (x^2 + y^2)^{1/2}$ ,  $k_F = M\pi/d$ , and we have now chosen the origin to lie on the upper surface of the film, so that the location of the impurity is  $-b\hat{\mathbf{z}}$ .

In Eq. (B1), for  $b \ll d$  and  $z \ll d$ , the sum over  $n'$  can be replaced by an integral:

$$\begin{aligned} \sum_{n'=1}^M \frac{1}{(k'_{\parallel})^{1/2}} \sin(k'_1 b) \sin(k'_1 z) e^{ik'_{\parallel} \rho} &= \frac{(k_F d)^{1/2}}{2\pi} \int_0^{\pi/2} d\theta' \sqrt{\sin\theta'} e^{ik_F \rho \sin\theta'} \{ \cos[k_F(z-b)\cos\theta'] - \cos[k_F(z+b)\cos\theta'] \} \\ &\simeq id \left[ \frac{\sin\theta}{2\pi r} \right]^{1/2} e^{-i\pi/4} e^{ik_F r} \sin(k_F z b / r), \end{aligned} \quad (\text{B2})$$

where  $r_{\parallel}/r = \sin\theta$ . Upon substituting Eqs. (B2) into (B1), the expression for  $\psi_{n\mathbf{k}}^{(+)}$  becomes

$$\begin{aligned} \psi_{n\mathbf{k}}^{(+)}(\mathbf{r}) = & (-1)^n \sqrt{2/\Omega} \sin(k_{\perp} z) e^{ik_{\parallel} r_{\parallel}} - 2i(-1)^n \sqrt{2/\Omega} \sin(k_{\perp} b) \sin(k_F z b / r) \\ & \times \left[ \frac{e^{-i\delta_0}}{\sin\delta_0} + ih_0^{(1)}(2k_F b) \right]^{-1} \frac{e^{ik_F r}}{k_F r}. \end{aligned} \quad (\text{B3})$$

Expression (B3) is the scattered state which was displayed in Ref. 6 for the case of an impurity near the metal surface of a semi-infinite medium in the quantum-mechanical asymptotic regime, where  $k_F r \gg 1$ .

We show that the resistivity for thin films, given by Eq. (45), can be extended to thick film case by the same trick: changing all the discrete sums into integrals. The sum in Eq. (45) becomes

$$\begin{aligned} \sum_{n=1}^M \sin^2(\pi b n / d) k_{Fn}^2 &= \frac{k_F^3 d}{\pi} \int_0^{\pi/2} \cos\theta \sin^2(k_F b \sin\theta) \cos^2\theta d\theta \\ &= \frac{k_F^3 d}{3\pi} \left[ 1 - \frac{3j_1(2k_F b)}{2k_F b} \right]. \end{aligned} \quad (\text{B4})$$

Again, only the  $j=0$  term is kept in  $A_0$  and  $B_0$ . The resulting resistivity is given by

$$\Delta\rho = \frac{\hbar}{e^2} \frac{12\pi^3}{k_F^4} \frac{n_i}{d} \text{Im} \left[ \left[ \frac{e^{-i\delta_0}}{\sin\delta_0} + ih_0^{(1)}(2k_F b) \right]^{-1} \right] \left[ 1 - \frac{3j_1(2k_F b)}{2k_F b} \right], \quad (\text{B5})$$

which was obtained in Ref. 6 for impurities near the surface of a semi-infinite medium.

<sup>1</sup>See, for example, *Localization, Interaction, and Transport Phenomena*, edited by B. Kramer, G. Bergmann, and Y. Bruynseraede (Springer-Verlag, New York, 1985).

<sup>2</sup>R. Landauer, IBM J. Res. Develop, **1**, 223 (1957).

<sup>3</sup>R. Landauer, Z. Phys. B **21**, 247 (1975).

<sup>4</sup>R. S. Sorbello and B. Dasgupta, Phys. Rev. B **16**, 5193 (1977).

<sup>5</sup>R. S. Sorbello, Phys. Rev. B **23**, 5119 (1981).

<sup>6</sup>R. S. Sorbello and C. S. Chu, IBM J. Res. Develop, **32**, 58 (1988).

<sup>7</sup>R. S. Sorbello and C. S. Chu, Superlatt. Microstruct. **3**, 467 (1987).

<sup>8</sup>R. Landauer, Philos. Mag. **21**, 863 (1970).

<sup>9</sup>See, for example, M. Ya. Azbel, Phys. Rev. B **28**, 4106 (1983), and references cited therein.

<sup>10</sup>M. Büttiker, Y. Imry, R. Landauer, and S. Pinhas, Phys. Rev. B **31**, 6207 (1985).

<sup>11</sup>H. B. Huntington, in *Diffusion in Solids*, edited by A. S. Nowick and J. J. Burton (Academic, New York, 1975), p. 303.

<sup>12</sup>P. Kumar and R. S. Sorbello, Thin Solid Films **25**, 25 (1975).

<sup>13</sup>R. Landauer and J. W. F. Woo, Phys. Rev. B **10**, 1266 (1974); R. Landauer, *ibid.* **14**, 1474 (1976); **16**, 4698 (1977).

<sup>14</sup>C. Bosvieux and J. Friedel, J. Phys. Chem. Solids **23**, 123 (1962); A. K. Das and R. E. Peierls, J. Phys. C **8**, 3348 (1975).

<sup>15</sup>W. L. Schaich, Phys. Rev. B **13**, 3350 (1976).

<sup>16</sup>L. J. Sham, Phys. Rev. B **12**, 3142 (1975).

<sup>17</sup>P. R. Rimbey and R. S. Sorbello, Phys. Rev. B **21**, 2150 (1980).

<sup>18</sup>R. E. Howard, L. D. Jackel, P. M. Mankiewich, W. J. Skocpol, Science **231**, 346 (1986).

<sup>19</sup>W. J. Skocpol, P. M. Mankiewich, R. E. Howard, L. D. Jackel, and D. M. Tennant, Phys. Rev. Lett. **56**, 2865 (1986).

<sup>20</sup>D. Stark and P. Zwicknagl, Appl. Phys. **21**, 397 (1980).

<sup>21</sup>J. Vancea, H. Hoffmann, and K. Kastner, Thin Solid Films **121**, 201 (1984).

<sup>22</sup>J. C. Hensel, R. T. Tung, J. M. Poate, and J. C. Unterwald, Phys. Rev. Lett. **54**, 1840 (1985).

<sup>23</sup>K. Fuchs, Proc. Cambridge Philos. Soc. **34**, 100 (1938).

<sup>24</sup>E. H. Sondheimer, Adv. Phys. **1**, 1 (1952).

<sup>25</sup>S. B. Soffer, J. Appl. Phys. **38**, 1710 (1967).

<sup>26</sup>K. L. Chopra, *Thin Film Phenomena* (McGraw-Hill, New York, 1969).

<sup>27</sup>R. F. Greene and R. W. O'Donnell, Phys. Rev. **147**, 599 (1966).

<sup>28</sup>M. Watanabe, J. Res. Inst. Catal. **26**, 107 (1978).

<sup>29</sup>K. M. Leung, Phys. Rev. B **30**, 647 (1984).

<sup>30</sup>Z. Tešanović, M. V. Jarić, and S. Maekawa, Phys. Rev. Lett. **57**, 2760 (1986).

<sup>31</sup>The transport equation with the term  $\overline{g_{\mathbf{k}}}/\tau$  is obtained rigorously by assuming the transition rate  $W_{\mathbf{k}\mathbf{k}'}$  in the collision integral is isotropic. The derivation is similar to that given in Sec. III C for the case of a thin film.

<sup>32</sup>E. D. Siggia and P. C. Kwok, Phys. Rev. B **2**, 1024 (1970).

<sup>33</sup>J. B. Pendry, *Low-Energy Electron Diffraction Theory* (Academic, London, 1974).

<sup>34</sup>The derivation of Eq. (17) is similar to the treatment of multiple scattering within a plane of ion cores as shown in Sec. IV C of Pendry's book (Ref. 33).

<sup>35</sup>The function  $G_{l',m',l,m}(\mathbf{x})$  enters the theory via the Eq. (4.38) in Penry's book (Ref. 33).

<sup>36</sup>All spherical and cylindrical special functions are defined the same way as in the book by J. D. Jackson, *Classical Electrodynamics* (Wiley, New York, 1975).

<sup>37</sup>See p. 467 of the book by P. M. Morse and H. Feshbach, *Methods of Theoretical Physics* (McGraw-Hill, New York, 1953).

<sup>38</sup>The largest mean free path cannot be greater than  $2l$  for any film thickness  $d$ . Since the mean free path  $l_n$  equals  $\hbar k_{Fn} \tau / m = l k_{Fn} / k_F$ , where  $k_F$  is the bulk Fermi wave vector of the electrons, the longest  $l_n$  must equal  $l_1$ . The expression for  $l_1$  is  $l [K_F^2(t) / k_F^2 - (1/t)^2]^{1/2}$ , where  $t \equiv k_F d / \pi$  and  $\hbar^2 K_F^2(t) / 2m$  is the Fermi energy. In the limit of one occupied subband,  $l_1$  can be expressed as  $l (2k_F d / 3\pi)^{1/2} \leq 1.05l$ . From Fig. 3 in the paper by Leung (Ref. 29), we deduce that  $l_1 < 2l$

for any film thickness  $d$ .

<sup>39</sup>N. Trivedi and N. W. Ashcroft (unpublished). These authors consider impurity scattering within the Born approximation and surface roughness within the model due to Tešanović *et al.* (Ref. 30). Their result for the resistivity shows oscillatory features similar to those in our Born-approximation re-

sult shown in Fig. 2(d).

<sup>40</sup>C. S. Chu and R. S. Sorbello (unpublished).

<sup>41</sup>R. Landauer and J. W. F. Woo, *Phys. Rev. B* **5**, 1189 (1972).

<sup>42</sup>R. S. Sorbello, *Phys. Rev. B* **31**, 798 (1985).

<sup>43</sup>R. Landauer, *Phys. Rev. B* **14**, 1474 (1976).